



6-2014

Effect of Toxic Metal on Root and Shoot Biomass of a Plant A Mathematical Model

O. P. Misra
Jiwaji University

Preety Kalra
Jiwaji University

Follow this and additional works at: <https://digitalcommons.pvamu.edu/aam>

 Part of the [Biology Commons](#), and the [Other Physical Sciences and Mathematics Commons](#)

Recommended Citation

Misra, O. P. and Kalra, Preety (2014). Effect of Toxic Metal on Root and Shoot Biomass of a Plant A Mathematical Model, *Applications and Applied Mathematics: An International Journal (AAM)*, Vol. 9, Iss. 1, Article 11.

Available at: <https://digitalcommons.pvamu.edu/aam/vol9/iss1/11>

This Article is brought to you for free and open access by Digital Commons @PVAMU. It has been accepted for inclusion in *Applications and Applied Mathematics: An International Journal (AAM)* by an authorized editor of Digital Commons @PVAMU. For more information, please contact hvkoshy@pvamu.edu.



Effect of Toxic Metal on Root and Shoot Biomass of a Plant A Mathematical Model

O.P. Misra and Preety Kalra

School of Mathematics and Allied Sciences

Jiwaji University

Gwalior, M.P., 474011, India

misra_op58@yahoo.co.in , kalra.preety@gmail.com

Received: January 11, 2013; Accepted: April 30, 2014

Abstract

In this paper, a mathematical model is proposed to study the impact of toxic metals on plant growth dynamics due to transfer of the toxic metal in plant tissues. In the model, it is assumed that the plant uptakes the metal from the soil through the roots and then it is transferred in the plant tissues and cells by transport mechanisms. It is observed experimentally that when toxic (heavy) metals combines with the nutrient they form a complex compound due to which nutrient loses its inherent properties and the natural characteristics of the nutrient are damaged. It is noticed that due to the presence of toxic (heavy) metal in the plant tissues and loss of inherent properties of nutrient due to reaction with the toxic metal, the growth rate of the plant decreases. In order to understand the impact on plant growth dynamics, we have studied two models: One model for a plant growth with no toxic effect and the other model for plant growth with toxic effect. From the analysis of the models the criteria for plant growth with and without toxic effects are derived. The numerical simulation to support the analytical results is done using MathLab.

Keywords: Nutrient Concentration; Root and Shoot Biomass; Toxic Metal; Model; Equilibria and Stability

AMS-MSC 2010 No.: 92B05, 92C80

1. Introduction

The soil is a source of nutrients for plant growth, but it also acts as a sink for contaminants from industrial and agricultural waste materials [Basta et al. (2005); Bolan et al. (2003); Nwachukwu

and Agbede (2009)]. Over the last few years, the level of heavy metals in the agricultural fields are increasing as a consequence of increasing environmental pollution from industrial, agricultural and municipal wastes. Plants take heavy metals from soils through different reactions such as: absorption, ionic exchange, redox reactions, precipitation–dissolution, etc. Heavy metals, through their action, disturb plant metabolism, affecting respiration, photosynthesis, stomata opening and plant growth. Heavy metals such as lead, copper, zinc, in high concentrations, are toxic to plants, preventing their proper development. Plants uptake metals from soil through their roots and then transport within the plant and plant cells [Smical et al. (2008)]. Plants accumulate heavy metals in their tissue and their high concentrations are toxic to them. In an experiment with maize it has been shown that the presence of Aluminum concentration in plant tissue has reduced the growth rate of the plant [Lindon and Barreiro (1998)]. It is observed experimentally that the heavy (toxic) metals (when they combine with nutrients) form a complex compound thereby destroying the inherent properties of the nutrients [Violante et al. (2010)].

Agricultural research almost completely rely upon experimental and empirical works, combined with statistical analysis so very few mathematical modelling analysis has been carried out in this direction [Leo et al. (1993); Verma et al. (2007); Gross (1990); Thornley (1976); Benjamin and Hardwick (1986); Pugliese (1988); Somma et al. (1988); Ittersum et al. (2002); Dercole et al. (2005); Ioslovich and Gautam (2005); Vance and Nevai (2007); DeAngelis and Gross (1992)]. Many of the models that have been used by agronomists and foresters to predict harvests and schedule fertilization, irrigation and pesticide application are of empirical form. A major limitation in all these approaches is the unpredictability of the environmental inputs [Gross (1990)]. Thornley initiated some work related to the mathematical modelling of individual plant growth processes in which the mathematical models were applied to a wide variety of topics in plant physiology [Thornley (1976)]. In the paper of [Verma (2007)], a study was conducted through mathematical models to understand the cadmium uptake by radish, carrot, spinach and cabbage. In this paper a dynamic macroscopic numerical model for heavy metal transport and its uptake by vegetables in the root zone is considered and analysed numerically. Some mathematical models to study the effects of toxic metal on plant growth do now exist [Verma et al. (2007); Gross (1990); Brune and Dietz (1985); Pishchik et al. (2002); Guala (2010); Thomas et al. (2005); Misra and Kalra (2012); Misra and Kalra (2013)].

Inspired by the above, therefore in this paper, a mathematical model is proposed in this paper to study the impact of toxic metals on plant growth dynamics due to the transfer of toxic metal in plant tissues.

2. Mathematical Model

For the purpose of modelling, the plant is divided into root and shoot compartments in which the state variables considered are nutrient concentration and biomass. In the model, it is assumed that

the plant uptake the metal from the soil through the roots and then transferred it through the plant tissues and cells by transport mechanisms. It is further assumed in the model that the root and shoot biomass decrease due to damage of tissues and cells on account of the metal present in the components of the plant. It is also assumed in the model that the nutrient concentration in the root and shoot compartments decrease due to the formation of complex compounds with toxic metal.

Model 1 (Model with no toxic effect)

In the formulation of model, the plant is divided into two compartments, viz., the root and shoot compartments. The state variables associated with the each compartment are the root biomass, shoot biomass and nutrient concentration. W_r and W_s denote the root biomass and shoot biomass, respectively. S_0 and S_1 denote the nutrient concentration in the root and shoot compartments respectively. Thus, to study the plant growth dynamics, the following model is proposed.

$$\frac{dS_0}{dt} = K_N - r(S_0)W_r + D_{10}(S_1 - S_0) - D_{20}(S_0 - S_1) - \delta_1 S_0, \quad (1)$$

$$\frac{dS_1}{dt} = uf_g(I, C_1) - r(S_1)W_s - D_{10}(S_1 - S_0) + D_{20}(S_0 - S_1) - \delta_2 S_1, \quad (2)$$

$$\frac{dW_r}{dt} = r(S_0) \left(W_r - \frac{\delta_r W_r^2}{k_{r0}} \right), \quad (3)$$

$$\frac{dW_s}{dt} = r(S_1) \left(W_s - \frac{\delta_s W_s^2}{k_{s0}} \right), \quad (4)$$

with the initial conditions as:

$$S_0(0) > 0, S_1(0) > 0, W_r(0) > 0, W_s(0) > 0,$$

where, K_N is the nutrient uptake by the plant root and considered independent of the amount of root-mycorrhizal surface and its uptake characteristics. $r(S_0)W_r$ and $r(S_1)W_s$ represent the use of the nutrient by the root and shoot compartments of the plant respectively (Thronley (1976)). In the present analysis we assume the following forms for function $r(S_0)$ and $r(S_1)$ [Thronley (1976); DeAngelis and Gross (1992)]:

$$\begin{aligned}
 r(S_0) &= \eta m_r \mu_r \frac{S_0}{K_r + S_0}, \quad r'(S_0) > 0 \text{ for } S_0 > 0, \\
 r(S_1) &= \eta m_s \mu_s \frac{S_1 e^{-S_1 \tau_1}}{K_s + S_1}, \quad r'(S_1) > 0 \text{ for } S_1 > 0, \text{ and} \\
 r(0) &= 0,
 \end{aligned} \tag{5}$$

where, η is the utilization coefficient. m_r and m_s are the proportion of total biomass allocated to root and shoot biomass respectively, μ_r and μ_s are the resource-saturated rates of resource uptake per unit of root and shoot biomass respectively, S is senescence constant, K_r and K_s are half saturation constants. In the absence of nutrient concentration the plant will not grow and eventually will die out. u is the fraction of shoot in the form of leaf tissue. $f_g(I, C_1)$ is the specific gross photosynthetic rate (Thornley, 1976) given.

$$f_g(I, C_1) = \frac{l\beta I \gamma C_1}{\beta I + \gamma C_1} e^{-S_p \tau_1}, \tag{6}$$

where, τ_1 is the maximum age of the shoot of plant. l is the specific leaf area of the whole plant. I is the light flux density incident on the leaves in the shoot compartment, C_1 is the CO_2 density and in plant. S_p is the rate of senescence of the photosynthesis. β is the photochemical efficiency and γ is the conductance to CO_2 . In plant growth, it is considered that during the initial stage, i.e., during the lag phase, the rate of plant growth is slow. Rate of growth then increases rapidly during the exponential phase. After some time the growth rate slowly decreases due to limitation of nutrient. This phase constitutes the stationary phase. The terms

$$r(S_0) \frac{\delta_r W_r^2}{k_{r0}} \text{ and } r(S_1) \frac{\delta_s W_s^2}{k_{s0}}$$

are taken as the diminishing growth phase and stationary phase in the plant growth dynamics. Where, k_{r0} is the maximum root biomass, k_{s0} is the maximum shoot biomass, δ_r and δ_s are nutrient limiting coefficients, $D_{10}(S_1 - S_0)$ and $D_{20}(S_0 - S_1)$ represent the flux of nutrient from shoot to root and root to shoot, respectively. D_{10} and D_{20} are transfer rates. $\delta_1 S_0$ represents the loss of nutrient due to leaching. $\delta_2 S_1$ represent the loss of nutrient due to shedding of leaves, where, δ_1 and δ_2 are rate constants.

Model 2 (Model with toxic effect)

Now, we consider the effect of toxic metal on plant growth dynamics by assuming that the growth of plant biomass is inhibited and reduced due to the presence of the toxic metal in the soil. Let $C(t)$ be the concentration of toxic metal in soil and $\theta_c(t)$ be the concentration of toxic

metal in plant root. After incorporating the effect of toxic metal in Model 1, the resulting model is given as follows:

$$\frac{dS_0}{dt} = K_N - r(S_0)W_r + D_{10}(S_1 - S_0) - D_{20}(S_0 - S_1) - \alpha_1 S_0 \theta_c - \delta_1 S_0, \quad (7)$$

$$\frac{dS_1}{dt} = uf_g(I, C_1) - r(S_1)W_s - D_{10}(S_1 - S_0) + D_{20}(S_0 - S_1) - \alpha_2 S_1 \theta_c - \delta_2 S_1, \quad (8)$$

$$\frac{dW_r}{dt} = r(S_0) \left(W_r - \frac{\delta_r W_r^2}{k_{r0}} \right) - \alpha_3 \beta_1 W_r, \quad (9)$$

$$\frac{dW_s}{dt} = r(S_1) \left(W_s - \frac{\delta_s W_s^2}{k_{s0}} \right) - \alpha_4 \beta_2 W_s, \quad (10)$$

$$\frac{dC}{dt} = Q_0 - \alpha C - \mu \rho K C, \quad (11)$$

$$\frac{d\theta_c}{dt} = \mu \rho K C - f \theta_c - h \theta_c, \quad (12)$$

with the initial conditions as:

$$S_0(0) > 0, S_1(0) > 0, W_r(0) > 0, W_s(0) > 0, C(0) > 0, \theta_c(0) > 0.$$

Here, Q_0 is the constant input rate of toxic metal which is considered independent of the amount of the root-mycorrhizal surface and its uptake characteristics. The term $\mu \rho K C$ represents the uptake of toxic metal by root from soil. where, μ is the first order rate constant. ρ is the soil bulk density. K is the linear absorption coefficient. The term $f \theta_c$ represents the transfer of toxic metal in the plant tissue (shoot tissue) and where f is the transfer rate of the toxic metal in the plant tissue. The terms $\alpha_3 \beta_1 W_r$ and $\alpha_4 \beta_2 W_s$ represent the decrease in the growth of the plant due to the presence of toxic metal in root and shoot, respectively; where, β_1 and β_2 represent the bioconcentration factors or bioavailability factors and are taken as follows [Nwachukwu and Agbede (2009); Smical et al. (2008)]:

$$\beta_1 = \frac{\theta_c}{C}, \beta_2 = \frac{f \theta_c}{\mu \rho K C}. \quad (13)$$

The terms $\alpha_1 S_0 \theta_c$ and $\alpha_2 S_1 \theta_c$ represent the decrease in the nutrient concentration in the root and shoot respectively due to the formation of complex compounds with toxic metal. α_1 and α_2 are reaction rates of S_0 and S_1 with θ_c respectively. h is the natural decay rate of θ_c due to soil

depletion on account of the natural process of leaching. α is the natural decay rate of C on account of leaching and other natural process. Here, all the parameters $K_N, D_{10}, D_{20}, \delta_1, \delta_2, \mu_r, \mu_s, \eta, K_r, K_s, S, \tau_1, u, l, I, C_1, \beta, \gamma, S_p, k_{r0}, k_{s0}, \delta_r, \delta_s, \alpha_1, \alpha_2, Q_0, \mu, \rho, k, \alpha, f, \beta_1, \beta_2, \alpha_3, \alpha_4$ and h are taken as positive constants.

3. Boundedness and Dynamical Behavior

3.1. Analysis of Model 1

Now, we show that the solutions of the model given by (1) to (4) are bounded in a positive orthant in R^4_+ . The boundedness of the solutions is given by the following lemma.

Lemma 3.1.

All the solutions of model will lie in the region

$$B_1 = \left\{ (S_0, S_1, W_r, W_s) \in R^4_+ : 0 \leq S_0 + S_1 \leq \frac{K_N + uf_g(I, C_1)}{\theta_1}, 0 \leq W_r \leq \frac{k_{r0}}{\delta_r}, 0 \leq W_s \leq \frac{k_{s0}}{\delta_s} \right\},$$

as $t \rightarrow \infty$, for all positive initial values $(S_0(0), S_1(0), W_r(0), W_s(0)) \in R^4_+$, where $\theta_1 = \min(\delta_1, \delta_2)$.

Proof:

By adding equations (1) and (2), we get

$$\frac{d(S_0 + S_1)}{dt} \leq K_N + uf_g(I, C_1) - \theta_1(S_0 + S_1),$$

where, $\theta_1 = \min(\delta_1, \delta_2)$ and then by the usual comparison theorem we get, as $t \rightarrow \infty$,

$$S_0 + S_1 \leq \frac{K_N + uf_g(I, C_1)}{\theta_1}.$$

From equation (3), we get,

$$\begin{aligned} \frac{dW_r}{dt} &\leq r(S_0)W_r \left(1 - \frac{\delta_r W_r}{k_{r0}} \right), \\ &\leq \eta m_r \mu_r W_r \left(1 - \frac{\delta_r W_r}{k_{r0}} \right). \end{aligned}$$

Then, by the usual comparison theorem we get, as $t \rightarrow \infty$,

$$W_r \leq \frac{k_{r0}}{\delta_r}.$$

Similarly from equation (4), we get

$$W_s \leq \frac{k_{s0}}{\delta_s}.$$

This completes the proof of lemma.

Now we show the existence of the interior equilibrium E^* of Model 1. The system of equations (1) - (4) has one feasible equilibria $E^*(S_0^*, S_1^*, W_r^*, W_s^*)$. The equilibrium E^* of the system is obtained by solving the following equations:

$$K_N - r(S_0^*)W_r^* + D_{10}(S_1^* - S_0^*) - D_{20}(S_0^* - S_1^*) - \delta_1 S_0^* = 0, \quad (14)$$

$$uf_g(I, C_1) - r(S_1^*)W_s^* - D_{10}(S_1^* - S_0^*) + D_{20}(S_0^* - S_1^*) - \delta_2 S_1^* = 0, \quad (15)$$

$$\delta_r W_r^* - k_{r0} = 0, \quad (16)$$

$$\delta_s W_s^* - k_{s0} = 0. \quad (17)$$

Thus, from the above set of equations we get the positive equilibrium $E^* = (S_0^*, S_1^*, W_r^*, W_s^*)$, where

$$W_r^* = \frac{k_{r0}}{\delta_r}, \quad (18)$$

$$W_s^* = \frac{k_{s0}}{\delta_s}, \quad (19)$$

and the positive value of S_0^* and S_1^* can be obtained by solving the following pair of equations:

$$F_1(S_0, S_1) = K_N - r(S_0) \frac{k_{r0}}{\delta_r} + D_{10}(S_1 - S_0) - D_{20}(S_0 - S_1) - \delta_1 S_0 = 0, \quad (20)$$

$$F_2(S_0, S_1) = K_N + uf_g(I, C_1) - r(S_0) \frac{k_{r0}}{\delta_r} - r(S_1) \frac{k_{s0}}{\delta_s} - \delta_1 S_0 - \delta_2 S_1 = 0. \quad (21)$$

From equations (20) and (21), we have:

1. $F_1(S_0, 0) = 0$ implies $f_{11}(S_0) = \delta_r l_{11} S_0^2 + (\eta m_r \mu_r k_{r0} + \delta_r (l_{11} K_r - K_N)) S_0 - K_r K_N = 0$,
2. $F_1(0, S_1) = 0$ implies $f_{12}(S_1) = K_N + (D_{10} + D_{20}) S_1 = 0$,
3. $F_2(S_0, 0) = 0$ implies $f_{21}(S_0) = \delta_r \delta_1 S_0^2 + (\eta m_r \mu_r k_{r0} + \delta_r (\delta_1 K_r - m)) S_0 - K_r \delta_r m = 0$,
4. $F_2(0, S_1) = 0$ implies $f_{22}(S_1) = \delta_s \delta_2 S_1^2 + (\eta m_s \mu_s k_{s0} + \delta_s (\delta_2 K_s - m)) S_1 - K_s \delta_s m = 0$,

where

$$l_{11} = D_{10} + D_{20} + \delta_1 \text{ and } m = K_N + uf_g(I, C_1).$$

The two equations (20) and (21) intersect each other in the positive phase plane satisfying $dS_1/dS_0 > 0$, for equation (20) and $dS_1/dS_0 < 0$, for equation (21), showing the existence of the unique interior equilibrium E^* .

From equation (15) as $\tau_1 \rightarrow \infty$:

$$S_1^* = \frac{(D_{10} + D_{20}) S_0^*}{D_{10} + D_{20} + \delta_2}. \quad (22)$$

Now, we discuss the dynamical behaviour of the interior equilibrium point E^* of the model given by (1)-(4) and for this local and global stability analysis have been carried out subsequently.

The characteristic equation associated with the variational matrix about equilibrium E^* is given by

$$(\lambda + P_4)(\lambda + P_5)(\lambda^2 + (P_1 + P_3)\lambda + P_1 P_3 - P_2^2) = 0, \quad (23)$$

where

$$P_1 = \frac{\eta m_r \mu_r K_r W_r^*}{(K_r + S_0)^2} + D_{10} + D_{20} + \delta_1, \quad P_2 = D_{10} + D_{20},$$

$$P_3 = \frac{\eta m_s \mu_s K_s W_s^* e^{-S_1^*}}{(K_s + S_1)^2} + D_{10} + D_{20} + \delta_2, \quad P_4 = \frac{r(S_0^*) W_r^*}{k_{r0}},$$

$$P_5 = \frac{r(S_1^*) W_s^*}{k_{s0}}, \quad P_1 P_3 - P_2^2 > 0.$$

From the nature of the roots of the characteristic equation (23) we derive that the equilibrium point E^* is always locally asymptotically stable.

Now, we discuss the global stability of the interior equilibrium point E^* of the system (1)-(4). The non-linear stability of the interior positive equilibrium is determined by the following theorem.

Theorem 3.2.

In addition to assumptions (5), let $r(S_0)$ and $r(S_1)$, satisfy in B_1

$$\begin{aligned} 0 \leq r(S_0) \leq \eta m_r \mu_r, \quad 0 \leq r'(S_0) \leq \eta m_r \mu_r K_r, \\ 0 \leq r(S_1) \leq \eta m_s \mu_s, \quad 0 \leq r'(S_1) \leq \eta m_s \mu_s K_s, \end{aligned} \quad (24)$$

for some positive constants K_r and K_s less than 1. Then, if the following inequalities hold

$$(D_{10} + D_{20})^2 < \left(\frac{\eta m_r \mu_r W_r^*}{K_r (1 + \eta m_r \mu_r)^2} + D_{10} + D_{20} + \delta_1 \right) \left(\frac{\eta m_s \mu_s W_s^*}{K_s (1 + \eta m_s \mu_s)^2} + D_{10} + D_{20} + \delta_2 \right), \quad (25)$$

$$\begin{aligned} \left[\eta m_r \mu_r \left(1 + \left(\frac{\eta m_r \mu_r K_r}{k_{r0}} - \frac{1}{K_r (1 + \eta m_r \mu_r)^2} \right) \right) \right]^2 \\ < 2 \left(\frac{\eta m_r \mu_r W_r^*}{K_r (1 + \eta m_r \mu_r)^2} + D_{10} + D_{20} + \delta_1 \right) \left(\frac{r(S_0^*) \delta_r}{k_{r0}} \right), \end{aligned} \quad (26)$$

$$\begin{aligned} \left[\eta m_s \mu_s \left(1 + \left(\frac{\eta m_s \mu_s K_s}{k_{s0}} - \frac{1}{K_s (1 + \eta m_s \mu_s)^2} \right) \right) \right]^2 \\ < 2 \left(\frac{\eta m_s \mu_s W_s^*}{K_s (1 + \eta m_s \mu_s)^2} + D_{10} + D_{20} + \delta_2 \right) \left(\frac{r(S_1^*) \delta_s}{k_{s0}} \right), \end{aligned} \quad (27)$$

E^* is globally asymptotically stable with respect to solutions initiating in the interior of the positive orthant.

Proof:

Since B_1 is an attracting region, and does not contain any invariant sets on the part of its boundary which intersect in the interior of R_+^4 , we restrict our attention to the interior of B_1 . We consider a positive definite function about E^*

$$V_1(S_0, S_1, W_r, W_s) = \frac{1}{2}(S_0 - S_0^*)^2 + \frac{1}{2}(S_1 - S_1^*)^2 + \left(W_r - W_r^* - W_r^* \ln \frac{W_r}{W_r^*} \right) + \left(W_s - W_s^* - W_s^* \ln \frac{W_s}{W_s^*} \right).$$

Then, the derivatives along solutions, \dot{V}_1 is given by

$$\begin{aligned} \dot{V}_1 &= (S_0 - S_0^*)(K_N - r(S_0)W_r + D_{10}(S_1 - S_0) - D_{20}(S_0 - S_1) - \delta_1 S_0) \\ &+ (S_1 - S_1^*)(uf_g(I, C') - r(S_1)W_s - D_{10}(S_1 - S_0) + D_{20}(S_0 - S_1) - \delta_2 S_1) \\ &+ \left(1 - \frac{W_r^*}{W_r} \right) W_r r(S_0) \left(1 - \frac{\delta_r W_r}{k_{r0}} \right) + \left(1 - \frac{W_s^*}{W_s} \right) W_s r(S_1) \left(1 - \frac{\delta_s W_s}{k_{s0}} \right). \end{aligned}$$

After some algebraic manipulations, this can be written as

$$\begin{aligned} \dot{V}_1 &= (S_0 - S_0^*)(K_N - r(S_0)W_r^* - (D_{10} + D_{20} + \delta_1)S_0) \\ &+ (S_1 - S_1^*)(uf_g(I, C') - r(S_1)W_s^* - (D_{10} + D_{20} + \delta_2)S_1) \\ &+ (W_r - W_r^*)r(S_0^*) \left(1 - \frac{\delta_r W_r}{k_{r0}} \right) + (W_s - W_s^*)r(S_1^*) \left(1 - \frac{\delta_s W_s}{k_{s0}} \right) \\ &+ (S_0 - S_0^*)(S_1 - S_1^*)2(D_{10} + D_{20}) - (S_0 - S_0^*)(W_r - W_r^*) \left[r(S_0) + \xi_1(S_0) \left(\frac{W_r \delta_r}{k_{r0}} - 1 \right) \right] \\ &- (S_1 - S_1^*)(W_s - W_s^*) \left[r(S_1) + \xi_2(S_1) \left(\frac{W_s \delta_s}{k_{s0}} - 1 \right) \right], \end{aligned}$$

where

$$\xi_1(S_0) = \begin{cases} (r(S_0) - r(S_0^*)) / (S_0 - S_0^*), & S_0 \neq S_0^*, \\ r'(S_0), & S_0 = S_0^*, \end{cases}$$

and

$$\xi_2(S_1) = \begin{cases} (r(S_1) - r(S_1^*)) / (S_1 - S_1^*), & S_1 \neq S_1^*, \\ r'(S_1), & S_1 = S_1^*. \end{cases}$$

Note from (24) and the mean value theorem that

$$\frac{\eta m_r \mu_r}{K_r (1 + \eta m_r \mu_r)^2} \leq |\xi_1(S_0)| \leq \eta m_r \mu_r K_r \quad \text{and} \quad \frac{\eta m_s \mu_s}{K_s (1 + \eta m_s \mu_s)^2} \leq |\xi_2(S_1)| \leq \eta m_s \mu_s K_s.$$

We know that

$$K_N - r(S_0)W_r^* - (D_{10} + D_{20} + \delta_1)S_0 = -(\xi_1(S_0)W_r^* + D_{10} + D_{20} + \delta_1)(S_0 - S_0^*),$$

$$uf_g(I, C') - r(S_1)W_s - (D_{10} + D_{20} + \delta_2)S_1 = -(\xi_2(S_1)W_s^* + D_{10} + D_{20} + \delta_2)(S_1 - S_1^*),$$

$$r(S_0^*) \left(1 - \frac{\delta_r W_{rs}}{k_{r0}} \right) = - \left(\frac{\delta_r r(S_0^*)}{k_{r0}} \right) (W_r - W_r^*),$$

$$r(S_1^*) \left(1 - \frac{\delta_s W_s}{k_{s0}} \right) = - \left(\frac{\delta_s r(S_1^*)}{k_{s0}} \right) (W_s - W_s^*).$$

Hence, \dot{V}_1 can be written as the sum of three quadratic forms,

$$\begin{aligned} \dot{V}_1 = & -\{(S_0 - S_0^*)^2 a_{11} + (S_1 - S_1^*)^2 a_{22} + (W_r - W_r^*)^2 a_{33} + (W_s - W_s^*)^2 a_{44} \\ & + (S_0 - S_0^*)(W_r - W_r^*) a_{13} - (S_0 - S_0^*)(S_1 - S_1^*) a_{12} + (S_1 - S_1^*)(W_s - W_s^*) a_{24}\}, \end{aligned}$$

where

$$a_{11} = (\xi_1(S_0)W_r^* + D_{10} + D_{20} + \delta_1), \quad a_{22} = (\xi_2(S_1)W_s^* + D_{10} + D_{20} + \delta_2),$$

$$a_{33} = \left(\frac{\delta_r r(S_0^*)}{k_{r0}} \right), \quad a_{44} = \left(\frac{\delta_s r(S_1^*)}{k_{s0}} \right),$$

$$a_{12} = 2(D_{10} + D_{20}), \quad a_{13} = \left[r(S_0) + \xi_1(S_0) \left(\frac{W_r \delta_r}{k_{r0}} - 1 \right) \right],$$

$$a_{24} = \left[r(S_1) + \xi_2(S_1) \left(\frac{W_s \delta_s}{k_{s0}} - 1 \right) \right].$$

By Sylvester's criteria, we find that \dot{V}_1 is negative definite if

$$a_{12}^2 < a_{11} a_{22}, \tag{28}$$

$$a_{13}^2 < 2a_{11} a_{33}, \tag{29}$$

and

$$a_{24}^2 < 2a_{22}a_{44} \quad (30)$$

hold. However, (25) implies (28), (26) implies (29) and (27) implies (30). Hence, \dot{V}_1 is negative definite and so V_1 is a Liapunov function with respect to E^* , whose domain contains B_1 , proving the theorem.

The above theorem shows, the system settles down to a steady state solution provided inequalities (25) to (27) hold.

3.2. Analysis of Model 2

Now, in the following we show that the solutions of model given by (7) to (12) are bounded in a positive orthant in R^6_+ . The boundedness of solutions is given by the following lemma.

Lemma 3.3.

All the solutions of model will lie in the region

$$B_2 = \left\{ (S_0, S_1, W_r, W_s, C, \theta_C) \in R^6_+ : 0 \leq S_0 + S_1 \leq \frac{K_N + uf_g(I, C_1)}{\theta_1}, 0 \leq W_r \leq \frac{k_{r0}}{\delta_r}, 0 \leq W_s \leq \frac{k_{s0}}{\delta_s}, \right. \\ \left. 0 \leq C \leq \frac{Q_0}{\alpha}, 0 \leq \theta_C \leq \frac{\mu\rho Q_0}{\alpha h} \right\},$$

as $t \rightarrow \infty$, for all positive initial values $(S_0(0), S_1(0), W_r(0), W_s(0), C(0), \theta_C(0)) \in R^6_+$, where $\theta_1 = \min(\delta_1, \delta_2)$.

Proof:

By adding equations (7) and (8), we get

$$\frac{d(S_0 + S_1)}{dt} \leq K_N + uf_g(I, C_1) - \theta_1(S_0 + S_1),$$

where $\theta_1 = \min(\delta_1, \delta_2)$ and then by the usual comparison theorem we get, as $t \rightarrow \infty$:

$$S_0 + S_1 \leq \frac{K_N + uf_g(I, C_1)}{\theta_1}.$$

From equation (9), we get

$$\begin{aligned}\frac{dW_r}{dt} &\leq r(S_0)W_r \left(1 - \frac{\delta_r W_r}{k_{r0}}\right) \\ &\leq \eta m_r \mu_r W_r \left(1 - \frac{\delta_r W_r}{k_{r0}}\right).\end{aligned}$$

Then, by the usual comparison theorem we get, as $t \rightarrow \infty$:

$$W_r \leq \frac{k_{r0}}{\delta_r}.$$

Similarly from equation (10), we get

$$W_s \leq \frac{k_{s0}}{\delta_s}.$$

From equation (11), we get

$$\frac{dC}{dt} \leq Q_0 - \alpha C.$$

Then, by the usual comparison theorem we get, as $t \rightarrow \infty$:

$$C \leq \frac{Q_0}{\alpha}.$$

From equation (12), we get,

$$\frac{d\theta_C}{dt} \leq \frac{\mu\rho K Q_0}{\alpha} - h\theta_C.$$

Then, by the usual comparison theorem we get, as $t \rightarrow \infty$:

$$\theta_C \leq \frac{\mu\rho K Q_0}{\alpha h}.$$

This complete the proof of the Lemma.

Now, we find the interior equilibrium \tilde{E} of Model 2. The system of equations (7) - (12) has one feasible equilibria $\tilde{E}(\tilde{S}_0, \tilde{S}_1, \tilde{W}_r, \tilde{W}_s, \tilde{C}, \tilde{\theta}_C)$. The equilibrium \tilde{E} of the system is obtained by solving the following equations,

$$K_N - r(\tilde{S}_0)\tilde{W}_r + D_{10}(\tilde{S}_1 - \tilde{S}_0) - D_{20}(\tilde{S}_0 - \tilde{S}_1) - \alpha_1\tilde{S}_0\tilde{\theta}_C - \delta_1\tilde{S}_0 = 0, \quad (31)$$

$$uf_g(I, C_1) - r(\tilde{S}_1)\tilde{W}_s - D_{10}(\tilde{S}_1 - \tilde{S}_0) + D_{20}(\tilde{S}_0 - \tilde{S}_1) - \alpha_2\tilde{S}_1\tilde{\theta}_C - \delta_2\tilde{S}_1 = 0, \quad (32)$$

$$r(\tilde{S}_0)\left(1 - \frac{\delta_r\tilde{W}_r}{k_{r0}}\right) - \alpha_3\beta_1 = 0, \quad (33)$$

$$r(\tilde{S}_1)\left(1 - \frac{\delta_s\tilde{W}_s}{k_{s0}}\right) - \alpha_4\beta_2 = 0, \quad (34)$$

$$Q_0 - \alpha\tilde{C} - \mu\rho K\tilde{C} = 0, \quad (35)$$

$$\mu\rho K\tilde{C} - f\tilde{\theta}_C - h\tilde{\theta}_C = 0. \quad (36)$$

Thus, from the above set of equations we get the positive equilibrium $\tilde{E} = (\tilde{S}_0, \tilde{S}_1, \tilde{W}_r, \tilde{W}_s, \tilde{C}, \tilde{\theta}_C)$, where

$$\tilde{W}_r = \frac{k_{r0}}{\delta_r} \left(1 - \frac{\beta_1\alpha_3}{r(\tilde{S}_0)}\right), \quad (37)$$

$$\tilde{W}_s = \frac{k_{s0}}{\delta_s} \left(1 - \frac{\beta_2\alpha_4}{r(\tilde{S}_1)}\right), \quad (38)$$

$$\tilde{C} = \frac{Q_0}{\alpha + \mu\rho K}, \quad (39)$$

$$\tilde{\theta}_C = \frac{\mu\rho K\tilde{C}}{f + h}. \quad (40)$$

The positive value of \tilde{S}_0 and \tilde{S}_1 can be obtained by solving the following pair of equations:

$$G_1(S_0, S_1) = K_N + \frac{k_{r0}\beta_1\alpha_3}{\delta_r} - r(S_0)\frac{k_{r0}}{\delta_r} + D_{10}(S_1 - S_0) - D_{20}(S_0 - S_1) - \alpha_1S_0\tilde{\theta}_C - \delta_1S_0 = 0, \quad (41)$$

$$G_2(S_0, S_1) = K_N + uf_g(I, C_1) + \frac{k_{r0}\beta_1\alpha_3}{\delta_r} + \frac{k_{s0}\beta_2\alpha_4}{\delta_s} - r(S_0)\frac{k_{r0}}{\delta_r} - r(S_1)\frac{k_{s0}}{\delta_s} - \alpha_1S_0\tilde{\theta}_C - \alpha_2S_1\tilde{\theta}_C - \delta_1S_0 - \delta_2S_1 = 0. \quad (42)$$

From equations (41) and (42), we have

1. $G_1(S_0, 0) = 0$ implies $g_{11}(S_0) = l_1 S_0^2 + (\eta m_r \mu_r k_{r0} + l_1 K_r - l_2) S_0 - K_r l_2 = 0$,
2. $G_1(0, S_1) = 0$ implies $g_{12}(S_1) = \delta_r K_N + k_{r0} \beta_1 \alpha_3 + (D_{10} + D_{20}) S_1 = 0$,
3. $G_2(S_0, 0) = 0$ implies $g_{21}(S_0) = l_3 S_0^2 + (\eta m_r \mu_r \delta_r k_{r0} + l_3 K_r - l_4) S_0 - K_r l_4 = 0$,
4. $G_2(0, S_1) = 0$ implies $g_{22}(S_1) = l_5 S_1^2 + (\eta m_s \mu_s \delta_s k_{s0} + (l_5 K_s - l_4) S_1 - K_s l_4 = 0$,

where

$$l_1 = \delta_r (D_{10} + D_{20} + \delta_1 + \alpha_1 \tilde{\theta}_C), l_2 = \delta_r K_N + k_{r0} \beta_1 \alpha_3, l_3 = (\delta_1 + \alpha_1 \tilde{\theta}_C) \delta_r \delta_s,$$

$$l_4 = (K_N + u f_g(I, C_1)) \delta_r \delta_s + k_{r0} \beta_1 \alpha_3 + k_{s0} \beta_2 \alpha_4 \text{ and } l_5 = (\delta_2 + \alpha_2 \tilde{\theta}_C) \delta_r \delta_s.$$

The two equations (41) and (42) intersect each other in the positive phase plane satisfying $dS_1/dS_0 > 0$, for equation (41) and $dS_1/dS_0 < 0$, for equation (42), showing the existence of the unique interior equilibrium \tilde{E} .

From equation (32), as $\tau_1 \rightarrow \infty$:

$$\tilde{S}_1 = \frac{(D_{10} + D_{20}) \tilde{S}_0}{D_{10} + D_{20} + \alpha_2 \tilde{\theta}_C + \delta_2}. \quad (43)$$

Now, we discuss the dynamical behaviour of the interior equilibrium point \tilde{E} of the model given by (7)-(12) and for this local and global stability analysis have been carried out subsequently.

The characteristic equation associated with the variational matrix about equilibrium \tilde{E} is given by

$$(\lambda + J_7)(\lambda + J_8)(\lambda^4 + a_1 \lambda^3 + a_2 \lambda^2 + a_3 \lambda + a_4) = 0, \quad (44)$$

where

$$a_1 = J_1 + J_2 + J_4 + J_6,$$

$$a_2 = J_1 J_2 - (D_{10} + D_{20})^2 + J_4 J_6 + (J_1 + J_2)(J_4 + J_6) - r(\tilde{S}_0) J_3 - r(\tilde{S}_1) J_5,$$

$$a_3 = (J_1 J_2 - (D_{10} + D_{20})^2 + J_1 + J_2) J_4 J_6 + (J_1 + J_2)(J_4 + J_6) - r(\tilde{S}_0) J_3 (J_2 + J_6) - r(\tilde{S}_1) J_5 (J_1 + J_4),$$

$$a_4 = (J_1 J_2 - (D_{10} + D_{20})^2) J_4 J_6 + r(\tilde{S}_0) J_3 J_2 J_6 - r(\tilde{S}_1) J_5 J_1 J_4 - r(\tilde{S}_0) J_3 r(\tilde{S}_1) J_5$$

and

$$\begin{aligned} J_1 &= \frac{\eta m_r \mu_r K_r \tilde{W}_r}{(K_r + \tilde{S}_0)^2} + D_{10} + D_{20} + \delta_1 + \alpha_1 \tilde{\theta}_C, & J_2 &= \frac{\eta m_s \mu_s K_s \tilde{W}_s e^{-S_1}}{(K_s + \tilde{S}_1)^2} + D_{10} + D_{20} + \alpha_2 \tilde{\theta}_C + \delta_2, \\ J_3 &= \frac{\beta_1 \alpha_3 \tilde{W}_r}{r(\tilde{S}_0)}, & J_4 &= \frac{\delta_r r(\tilde{S}_0) \tilde{W}_r}{k_{r0}}, \\ J_5 &= \frac{\beta_2 \alpha_4 \tilde{W}_s}{r(\tilde{S}_1)}, & J_6 &= \frac{\delta_s r(\tilde{S}_1) \tilde{W}_s}{k_{s0}}, \\ J_7 &= \alpha + \mu \rho K, & J_8 &= f + h. \end{aligned}$$

From the Routh-Hurwitz's criteria it is found that \tilde{E} is locally asymptotically stable if $a_1 > 0, a_2 > 0, a_3 > 0, a_4 > 0$ and $a_1 a_2 a_3 - a_1^2 a_4 - a_3^2 > 0$.

Now, we discuss the global stability of the interior equilibrium point \tilde{E} of the system (7)-(12). The non-linear stability of the interior positive equilibrium state is determined by the following theorem.

Theorem 3.4.

In addition to assumptions (5), let $r(S_0)$ and $r(S_1)$ satisfy in B_2 ,

$$\begin{aligned} 0 \leq r(S_0) \leq \eta m_r \mu_r, \quad 0 \leq r'(S_0) \leq \eta m_r \mu_r K_r, \\ 0 \leq r(S_1) \leq \eta m_s \mu_s, \quad 0 \leq r'(S_1) \leq \eta m_s \mu_s K_s, \end{aligned} \quad (46)$$

for some positive constants K_r and K_s less than 1. Then, if the following inequalities hold

$$\begin{aligned} [(A_1 + A_2)(D_{10} + D_{20})]^2 &< \frac{4}{9} A_1 A_2 \left(\frac{\eta m_r \mu_r \tilde{W}_r}{K_r (1 + \eta m_r \mu_r)^2} + D_{10} + D_{20} + \alpha_1 \tilde{\theta}_C + \delta_1 \right) \\ &\cdot \left(\frac{\eta m_s \mu_s \tilde{W}_s}{K_s (1 + \eta m_s \mu_s)^2} + D_{10} + D_{20} + \alpha_2 \tilde{\theta}_C + \delta_2 \right), \end{aligned} \quad (47)$$

$$\begin{aligned} \left[\eta m_r \mu_r \left(A_1 + A_3 \left(\frac{\eta m_r \mu_r K_r}{k_{r0}} - \frac{1}{K_r (1 + \eta m_r \mu_r)^2} \right) \right) \right]^2 \\ < \frac{4}{9} A_1 A_3 \left(\frac{\eta m_r \mu_r \tilde{W}_r}{K_r (1 + \eta m_r \mu_r)^2} + D_{10} + D_{20} + \alpha_1 \tilde{\theta}_C + \delta_1 \right) \left(\frac{r(\tilde{S}_0) \delta_r}{k_{r0}} \right), \end{aligned} \quad (48)$$

$$\left[\eta m_s \mu_s \left(A_2 + A_4 \left(\frac{\eta m_s \mu_s K_s}{k_{s0}} - \frac{1}{K_s (1 + \eta m_s \mu_s)^2} \right) \right) \right]^2 < \frac{4}{9} A_2 A_4 \left(\frac{\eta m_s \mu_s \tilde{W}_s}{K_s (1 + \eta m_s \mu_s)^2} + D_{10} + D_{20} + \alpha_2 \tilde{\theta}_C + \delta_2 \right) \left(\frac{r(\tilde{S}_1) \delta_s}{k_{s0}} \right), \quad (49)$$

$$\left[A_3 \alpha_3 \tilde{\theta}_C \zeta_1(C) \right]^2 < \frac{4}{9} A_5 A_3 \left(\frac{\eta m_r \mu_r \tilde{W}_r}{K_r (1 + \eta m_r \mu_r)^2} + D_{10} + D_{20} + \alpha_1 \tilde{\theta}_C + \delta_1 \right) (\alpha + \mu \rho K), \quad (50)$$

$$\left[A_4 \alpha_4 \frac{f \tilde{\theta}_C}{\mu \rho K} \zeta_1(C) \right]^2 < \frac{4}{9} A_5 A_4 \left(\frac{\eta m_s \mu_s \tilde{W}_s}{K_s (1 + \eta m_s \mu_s)^2} + D_{10} + D_{20} + \alpha_2 \tilde{\theta}_C + \delta_2 \right) (\alpha + \mu \rho K). \quad (51)$$

\tilde{E} is globally asymptotically stable with respect to solutions initiating in the interior of the positive orthant.

Proof:

Since B_2 is an attracting region, and does not contain any invariant sets on the part of its boundary which intersect in the interior of R_+^6 , we restrict our attention to the interior of B_2 .

We consider a positive definite function about \tilde{E}

$$V_2(S_0, S_1, W_r, W_s, C, \theta_C) = \frac{1}{2} A_1 (S_0 - \tilde{S}_0)^2 + \frac{1}{2} A_2 (S_1 - \tilde{S}_1)^2 + A_3 \left(W_r - \tilde{W}_r - \tilde{W}_r \ln \frac{W_r}{\tilde{W}_r} \right) + A_4 \left(W_s - \tilde{W}_s - \tilde{W}_s \ln \frac{W_s}{\tilde{W}_s} \right) + \frac{1}{2} A_5 (C - \tilde{C})^2 + \frac{1}{2} (\theta_C - \tilde{\theta}_C)^2,$$

where, $A_i (i = 1, 2, 3, 4, 5)$ are arbitrary positive constants.

Then, the derivatives along the solutions, \dot{V}_2 is given by

$$\dot{V}_2 = A_1 (S_0 - \tilde{S}_0) (K_N - r(S_0) W_r + D_{10} (S_1 - S_0) - D_{20} (S_0 - S_1) - \alpha_1 S_0 \theta_C - \delta_1 S_0) + A_2 (S_1 - \tilde{S}_1) (u f_g(I, C') - r(S_1) W_s - D_{10} (S_1 - S_0) + D_{20} (S_0 - S_1) - \alpha_2 S_1 \theta_C - \delta_2 S_1)$$

$$\begin{aligned}
& + A_3 \left(1 - \frac{\tilde{W}_r}{W_r} \right) W_r \left[r(S_0) \left(1 - \frac{\delta_r W_r}{k_{r0}} \right) - \alpha_3 \frac{\theta_c}{C} \right] \\
& + A_4 \left(1 - \frac{\tilde{W}_s}{W_s} \right) W_s \left[r(S_1) \left(1 - \frac{\delta_s W_s}{k_{s0}} \right) - \alpha_4 \frac{f \theta_c}{\mu \rho K C} \right] \\
& + A_5 (C - \tilde{C}) (Q_0 - \alpha C - \mu \rho k C) + (\theta_c - \tilde{\theta}_c) (\mu \rho k C - f \theta_c - h \theta_c).
\end{aligned}$$

After some algebraic manipulations, this can be written as

$$\begin{aligned}
\dot{V}_2 = & A_1 (S_0 - \tilde{S}_0) (K_N - r(S_0) \tilde{W}_r - (D_{10} + D_{20} + \alpha_1 \tilde{\theta}_c + \delta_1) S_0) \\
& + A_2 (S_1 - \tilde{S}_1) (u f_g(I, C') - r(S_1) \tilde{W}_s - (D_{10} + D_{20} + \alpha_2 \tilde{\theta}_c + \delta_2) S_1) \\
& + A_3 (W_r - \tilde{W}_r) \left[r(\tilde{S}_0) \left(1 - \frac{\delta_r W_r}{k_{r0}} \right) - \alpha_3 \frac{\tilde{\theta}_c}{\tilde{C}} \right] \\
& + A_4 (W_s - \tilde{W}_s) \left[r(\tilde{S}_1) \left(1 - \frac{\delta_s W_s}{k_{s0}} \right) - \alpha_4 \frac{f \tilde{\theta}_c}{\mu \rho K \tilde{C}} \right] \\
& + A_5 (C - \tilde{C}) (Q_0 - \alpha C - \mu \rho K C) + (\theta_c - \tilde{\theta}_c) (-f \theta_c - h \theta_c) \\
& + (S_0 - \tilde{S}_0) (S_1 - \tilde{S}_1) (A_1 + A_2) (D_{10} + D_{20}) - A_1 (S_0 - \tilde{S}_0) (\theta_c - \tilde{\theta}_c) \alpha_1 S_0 \\
& - A_2 (S_1 - \tilde{S}_1) (\theta_c - \tilde{\theta}_c) \alpha_2 S_1 - (S_0 - \tilde{S}_0) (W_r - \tilde{W}_r) \\
& \quad \cdot \left[A_1 r(S_0) + A_3 \xi_1(S_0) \left(\frac{W_r \delta_r}{k_{r0}} - 1 \right) \right] \\
& - (S_1 - \tilde{S}_1) (W_s - \tilde{W}_s) \left[A_2 r(S_1) + A_4 \xi_2(S_1) \left(\frac{W_s \delta_s}{k_{s0}} - 1 \right) \right] \\
& + (\theta_c - \tilde{\theta}_c) (C - \tilde{C}) \mu \rho K \\
& - (\theta_c - \tilde{\theta}_c) (W_r - \tilde{W}_r) A_3 \frac{\alpha_3}{C} - (W_r - \tilde{W}_r) (C - \tilde{C}) A_3 \alpha_3 \tilde{\theta}_c \zeta_1(C) \\
& - (\theta_c - \tilde{\theta}_c) (W_s - \tilde{W}_s) A_4 \frac{\alpha_4}{C} \\
& - (W_s - \tilde{W}_s) (C - \tilde{C}) A_4 \alpha_4 \frac{f \tilde{\theta}_c}{\mu \rho K} \zeta_1(C),
\end{aligned}$$

where,

$$\xi_1(S_0) = \begin{cases} (r(S_0) - r(\tilde{S}_0)) / (S_0 - \tilde{S}_0), & S_0 \neq \tilde{S}_0, \\ r'(S_0), & S_0 = \tilde{S}_0, \end{cases}$$

$$\xi_2(S_1) = \begin{cases} (r(S_1) - r(S_1^*)) / (S_1 - S_1^*), & S_1 \neq S_1^*, \\ r'(S_1), & S_1 = S_1^*, \end{cases}$$

and

$$\zeta_1(C) = \begin{cases} \left(\frac{1}{C} - \frac{1}{\tilde{C}} \right) / (C - \tilde{C}), & C \neq \tilde{C}, \\ \frac{-1}{C^2}, & C = \tilde{C}. \end{cases}$$

Note from (46) and the mean value theorem that

$$\frac{\eta m_r \mu_r}{K_r (1 + \eta m_r \mu_r)^2} \leq |\xi_1(S_0)| \leq \eta m_r \mu_r K_r, \quad \frac{\eta m_s \mu_s}{K_s (1 + \eta m_s \mu_s)^2} \leq |\xi_2(S_1)| \leq \eta m_s \mu_s K_s \text{ and}$$

$$\frac{Q_0}{\alpha^2 + \mu \rho K} \leq |\zeta_1(C)| \leq \frac{Q_0}{\alpha}.$$

We know that

$$K_N - r(S_0) \tilde{W}_r - (D_{10} + D_{20} + \alpha_1 \tilde{\theta}_C + \delta_1) S_0 = -(\xi_1(S_0) \tilde{W}_r + D_{10} + D_{20} + \alpha_1 \tilde{\theta}_C + \delta_1)(S_0 - \tilde{S}_0),$$

$$\begin{aligned} u f_g(I, C') - r(S_1) W_s - (D_{10} + D_{20} + \alpha_2 \tilde{\theta}_C + \delta_2) S_1 \\ = -(\xi_2(S_1) \tilde{W}_s + D_{10} + D_{20} + \alpha_2 \tilde{\theta}_C + \delta_2)(S_1 - \tilde{S}_1), \end{aligned}$$

$$r(\tilde{S}_0) \left(1 - \frac{\delta_r W_r}{k_{r0}} \right) = - \left(\frac{\delta_r r(\tilde{S}_0)}{k_{r0}} \right) (W_r - \tilde{W}_r),$$

$$r(\tilde{S}_1) \left(1 - \frac{\delta_s W_s}{k_{s0}} \right) = - \left(\frac{\delta_s r(\tilde{S}_1)}{k_{s0}} \right) (W_s - \tilde{W}_s),$$

$$(Q_0 - \alpha C - \mu \rho K C) = -(\alpha + \mu \rho K)(C - \tilde{C}),$$

$$(-f \theta_C - h \theta_C) = -(\theta_C - \tilde{\theta}_C)(h + f).$$

Hence, \dot{V}_2 can be written as the sum of three quadratic forms,

$$\begin{aligned} \dot{V}_2 = & -\{(S_0 - \tilde{S}_0)^2 a_{11} + (S_1 - \tilde{S}_1)^2 a_{22} + (W_r - \tilde{W}_r)^2 a_{33} + (W_s - \tilde{W}_s)^2 a_{44} \\ & + (C - \tilde{C})^2 a_{55} + (\theta_C - \tilde{\theta}_C)^2 a_{66} - (S_0 - \tilde{S}_0)(S_1 - \tilde{S}_1) a_{12} + (S_0 - \tilde{S}_0)(\theta_C - \tilde{\theta}_C) a_{16} \} \end{aligned}$$

$$\begin{aligned}
&+(S_1 - \tilde{S}_1)(\theta_C - \tilde{\theta}_C)a_{26} + (S_0 - \tilde{S}_0)(W_r - \tilde{W}_r)a_{13} \\
&+(S_1 - \tilde{S}_1)(W_s - \tilde{W}_s)a_{24} - (\theta_C - \tilde{\theta}_C)(C - \tilde{C})a_{56} \\
&+(\theta_C - \tilde{\theta}_C)(W_r - \tilde{W}_r)a_{36} + (\theta_C - \tilde{\theta}_C)(W_s - \tilde{W}_s)a_{46} + (C - \tilde{C})(W_r - \tilde{W}_r)a_{35} \\
&+(C - \tilde{C})(W_s - \tilde{W}_s)a_{45}\},
\end{aligned}$$

where

$$\begin{aligned}
a_{11} &= A_1(\xi_1(S_0)\tilde{W}_r + D_{10} + D_{20} + \alpha_1\tilde{\theta}_C + \delta_1), & a_{22} &= A_2(\xi_2(S_1)\tilde{W}_s + D_{10} + D_{20} + \alpha_2\tilde{\theta}_C + \delta_2), \\
a_{33} &= A_3\left(\frac{\delta_r r(\tilde{S}_0)}{k_{r0}}\right), & a_{44} &= A_4\left(\frac{\delta_s r(\tilde{S}_1)}{k_{s0}}\right), \\
a_{55} &= A_5(\alpha + \mu\rho K), & a_{66} &= h + f, \\
a_{12} &= (A_1 + A_2)(D_{10} + D_{20}), & a_{13} &= \left[A_1 r(S_0) + A_3 \xi_1(S_0) \left(\frac{W_r \delta_r}{k_{r0}} - 1 \right) \right], \\
a_{16} &= A_1 \alpha_1 S_0, & a_{24} &= \left[A_2 r(S_1) + A_4 \xi_2(S_1) \left(\frac{W_s \delta_s}{k_{s0}} - 1 \right) \right], \\
a_{26} &= A_2 \alpha_2 S_1, & a_{36} &= A_3 \frac{\alpha_3}{C}, \\
a_{46} &= A_4 \frac{\alpha_4}{C}, & a_{35} &= A_3 \alpha_3 \tilde{\theta}_C \zeta_1(C), \\
a_{45} &= A_4 \alpha_4 \frac{f \tilde{\theta}_C}{\mu\rho K} \zeta_1(C), & a_{56} &= \mu\rho K.
\end{aligned}$$

By Sylvester's criteria we find that V_2 is negative definite if

$$\begin{aligned}
a_{12}^2 &< \frac{4}{9} a_{11} a_{22}, & a_{13}^2 &< \frac{4}{9} a_{11} a_{33}, & a_{16}^2 &< \frac{4}{15} a_{11} a_{66}, & a_{26}^2 &< \frac{4}{15} a_{22} a_{66}, \\
a_{24}^2 &< \frac{4}{9} a_{22} a_{44}, & a_{36}^2 &< \frac{4}{15} a_{33} a_{66}, & a_{46}^2 &< \frac{4}{15} a_{44} a_{66}, & a_{56}^2 &< \frac{4}{15} a_{55} a_{66}, \\
a_{35}^2 &< \frac{4}{9} a_{33} a_{55}, & a_{45}^2 &< \frac{4}{9} a_{44} a_{55},
\end{aligned} \tag{52}$$

hold. We note that inequalities in Equation (51), i.e., $a_{16}^2 < \frac{4}{15} a_{11} a_{66}$, $a_{26}^2 < \frac{4}{15} a_{22} a_{66}$, $a_{36}^2 < \frac{4}{15} a_{33} a_{66}$, $a_{46}^2 < \frac{4}{15} a_{44} a_{66}$ and $a_{56}^2 < \frac{4}{15} a_{55} a_{66}$ are satisfied due to arbitrary choice of A_1, A_2, A_3, A_4 and A_5 , respectively, and above conditions reduces to the following conditions:

$$a_{12}^2 < \frac{4}{9} a_{11} a_{22}, \tag{53}$$

$$a_{13}^2 < \frac{4}{9} a_{11} a_{33}, \tag{54}$$

$$a_{24}^2 < \frac{4}{9} a_{22} a_{44}, \quad (55)$$

$$a_{35}^2 < \frac{4}{9} a_{33} a_{55}, \quad (56)$$

$$a_{45}^2 < \frac{4}{9} a_{44} a_{55}. \quad (57)$$

However, (47) implies (53), (48) implies (54), (49) implies (55), (50) implies (56) and (51) implies (57). Hence, \dot{V}_2 is negative definite and so V_2 is a Liapunov function with respect to \tilde{E} , whose domain contains B_2 , proving the theorem.

The above theorem shows, the system settles down to a steady state solution provided inequalities (47) to (51) hold.

4. Numerical Example

For the model 1, consider the following values of parameters-

$$\begin{aligned} K_N = 10, & \quad K_s = 1, & \quad K_r = 1, & \quad \mu_s = 1.5, & \quad \mu_r = 1.2, \\ \eta = 4, & \quad m_r = 0.1, & \quad m_s = 0.1, & \quad D_{10} = 3, & \quad D_{20} = 5, \\ S = 0.01, & \quad \tau_1 = 90, & \quad k_{s0} = 20, & \quad k_{r0} = 20, & \quad u = 0.5, \\ l = 30, & \quad \beta = 0.1, & \quad \gamma = 1, & \quad C_1 = 0.374, & \quad I = 5, \\ S_p = 0.014, & \quad \delta_r = 1.2, & \quad \delta_s = 1.4, & \quad \delta_1 = 0.1, & \quad \delta_2 = 0.2. \end{aligned}$$

For the above set of parametric values, we obtain the following values of interior equilibrium E^*

$$S_0^* = 4.92, \quad S_1^* = 4.56, \quad W_r^* = 16.67, \quad W_s^* = 14.29,$$

which is asymptotically stable (see Figure 1).

Further, to illustrate the global stability of interior equilibrium E^* of model 1 graphically, numerical simulation is performed for different initial conditions (see Table 1 and 2) and results are shown in Figures 2 and 3 for $S_0 - W_r$ phase plane and $S_1 - W_s$ phase plane respectively. All the trajectories are starting from different initial conditions and reach to interior equilibrium E^* .

Table 1. Different initial conditions for S_0 and W_r of Model 1

$S_0(0)$	0.1	12	25	8
$W_r(0)$	2	0.1	25	30

Table 2. Different initial conditions for S_1 and W_s of Model 1

$S_1(0)$	0.1	4	25	10
$W_s(0)$	5	0.1	25	30

For the Model 2, with above set of parametric values and with the additional values of parameters given by

$$\alpha_1 = 1.8, \quad \alpha_2 = 2, \quad \mu = 1, \quad \rho = 2.5, \quad h = 2.5,$$

$$K = 0.75, \quad f = 0.8, \quad Q_0 = 12, \quad \alpha = 1, \quad \alpha_3 = 0.1,$$

$$\alpha_4 = 0.1,$$

we obtain the following values of interior equilibrium \tilde{E} as

$$\tilde{S}_0 = 0.95, \quad \tilde{S}_1 = 0.58, \quad \tilde{W}_r = 12.61, \quad \tilde{W}_s = 10.43, \quad \tilde{C} = 4.17, \quad \tilde{\theta}_C = 2.37.$$

For these set of parametric values, the stability conditions given in Equations (47)-(51) are satisfied. Hence, \tilde{E} is asymptotically stable (see Figure 4).

Further, to illustrate the global stability of interior equilibrium \tilde{E} of model 2 graphically, numerical simulation is performed for different initial conditions (see Table 3 and 4) and results are shown in Figures 5 and 6 for $S_0 - W_r$ phase plane and $S_1 - W_s$ phase plane respectively. All the trajectories are starting from different initial conditions and reach to interior equilibrium \tilde{E} .

Table 3. Different initial conditions for S_0 and W_r of Model 2

$S_0(0)$	0.1	2	2	0.6
$W_r(0)$	6	0.1	16	20

Table 4. Different initial conditions for S_1 and W_s of model 2

$S_1(0)$	0.1	1	1.3	0.2
$W_s(0)$	6	0.1	14	16

Tolerance indices (T.I.) are determined through the use of following formula [Kabir et al. (2008)]:

$$T.I.(root) = \frac{\text{Mean root mass in presence of toxicant}}{\text{Mean root mass in absence of toxicant}} \cdot 100$$

$$T.I.(shoot) = \frac{\text{Mean shoot mass in presence of toxicant}}{\text{Mean shoot mass in absence of toxicant}} \cdot 100$$

Table 5. Tolerance indices of root mass and shoot mass at different toxic input rate Q_0 when $f = 0.8$

S.No.	Q_0	W_r	W_s	T.I (W_r)%	T.I(W_s)%
1	0	16.6667	14.2857	100	100
2	1	14.1207	12.3998	84.76	86.79
3	5	13.4270	11.6459	80.56	81.52
4	10	12.8228	10.7818	76.93	75.47
5	15	12.3166	9.9020	73.89	69.31
6	20	11.8603	8.9253	71.15	62.48
7	25	11.4345	7.8006	68.60	54.60
8	30	11.0295	6.4758	66.17	45.30
9	35	10.6385	5.0461	63.82	35.32
10	40	10.2569	3.7212	61.49	26.05
11	45	9.8819	2.6627	59.27	18.64
12	50	9.5123	1.8989	57.07	13.29
13	60	8.7856	1.0211	52.71	7.15
14	70	8.0691	0.6121	48.41	4.28
15	100	5.8564	0.2245	35.13	1.57

Table 6. Bioavailability factors or bioconcentration factors β_1 and β_2 at different value of f when $Q_0 = 15$

F	W_r	W_s	C	θ_c	β_1	β_2
0.1	10.72	13.44	5.22	3.76	0.72	0.04
0.2	11.00	12.72	5.22	3.62	0.69	0.07
0.3	11.27	12.09	5.22	3.49	0.67	0.11
0.4	11.51	11.53	5.22	3.37	0.65	0.14
0.5	11.74	11.05	5.22	3.26	0.63	0.17
0.6	11.94	10.62	5.22	3.15	0.60	0.19
0.7	12.14	10.23	5.22	3.05	0.59	0.22
0.8	12.31	09.89	5.22	2.96	0.57	0.24
0.9	12.48	09.58	5.22	2.87	0.55	0.26

5. Conclusion

From Figures 7(a) and 7(b), it is observed that the equilibrium levels of nutrient concentrations in each compartment with no toxic effect are more than that of the equilibrium levels of nutrient concentrations in respective compartments when toxic effect is considered. Further, from Figures 8(a) and 8(b), it is observed that the equilibrium levels of root biomass and shoot biomass with no toxic effect are more than those of the root biomass and shoot biomass when toxic effect is being considered. From the non-trivial positive equilibrium \tilde{E} (Table 5), it is concluded that the root biomass and shoot biomass decrease as the input rate of toxic metal Q_0 increases and this phenomena will continue till Q_0 reaches $Q_{th} = 60$ because upto this value of Q_0 , the stability criteria continue to hold. From table 6, it is observed that as the transfer rate of toxic metal from root to shoot increases, toxicant concentration factor in root tissues decreases and consequently root biomass increases. On the contrary, toxicant concentration factor in shoot tissues increases as the transfer rate increases causing a decline of the shoot biomass. Figures 9(a) and 9(b) represent the dynamical behaviour of the nutrient concentration of root and shoot with respect to θ_c . From these figures, it is observed that nutrient concentration in root and shoot decrease as the level of the toxic metal concentration in root increases.

REFERENCES

- Brune, A. and Dietz, K. J. (1985). A Comparative Analysis of Element Composition of Roots and Leaves of Barley Seedlings Grown in the Presence of Toxic Cadmium, Molybdenum, Nickel and zinc Concentration, *J. Plant. Nutr.*, Vol. 18, 853-868.
- Benjamin, L. R. and Hardwick, R. C. (1986). Sources of Variation and Measures of Variability in Even-Aged Stands of Plants, *Ann. Bot.*, Vol. 58, 757-778.
- Bolan, N.S., Adriano, D.C., Natesa, R. and Koo, B.J. (2003). Effects of Organic Amendments on the Reduction and Phyto Availability of Chromate in Mineral Soil. *Journal of Environmental Quality*, Vol. 32, 120-128.
- Basta, N.T., J.A. Ryan and Chaney, R.L. (2005). Trace Element Chemistry in Residual Treated Soil: Key Concepts and Metal Bioavailability, *Journal of Environmental Quality*, Vol. 34, 49-63.
- DeAngelis, D. L. and Gross, L.J. (1992). Individual Based Models and Approaches in Ecology: Populations, *Communities and Ecosystems*, Chapman and Hall, New York, London.
- Dercole, F., Niklas, K., R. and Rand, R. (2005). Self-Thinning and Community Persistence in a Simple Size-Structure Dynamical Model of Plant Growth, *J. Math. Biol.*, Vol. 51, 333-354.
- Gross, L. J. (1990). Mathematical Modelling in Plant Biology: Implications of Physiological Approaches for Resource Management, *Third Autumn Course on Mathematical Ecology*, (International Center for Theoretical Physics, Trieste, Italy).

- Guala, S.D., Vega, F.A. and Coveló, E.F. (2010). The Dynamics of Heavy Metals in Plants – Soil Interaction, *Ecological Modelling*, Vol. 221, 1148-1152.
- Ittersum, M. K. V., Leffelaar, P.A., Keulen, H. V., Kropff, M. J., Bastiaans, L. and Goudriaan, J.(2002). Developments in Modelling Crop Growth, *Cropping Systems and Production Systems in the Wageningen School*, NJAS 50 .
- Ioslovich, I. and Gautam, P. (2005). On the Botanic Model of Plant Growth Intermediate Vegetative-Reproductive Stage, *Theoretical Population Biology*, Vol. 68, 147-156.
- Kabir, M., Zafar Iqbal, M., Shafiq, M., Farooqi, Z.R. (2008). Reduction in Germination and Seedling Growth of *Thespesia Populena* L., Caused by Lead and Cadmium Treatments, *Pak. J. Bot.*, Vol. 40, 2419-2426.
- Leo, G.D, Furia, L.D. and Gatto, M. (1993). The Interaction Between Soil Acidity and Forest Dynamics: A Simple Model Exhibiting Catastrophic Behavior, *Theoretical Population Biology*, Vol. 43, 31-51.
- Lindon, F.C. and Barreiro, M.G. (1998). Threshold Aluminum Toxicity in Maize, *Journal of Plant Nutrition* 21(3), 413-419.
- Misra, O.P. and Kalra, P. (2012). Modelling Effect of Toxic Metal on the Individuals Plant Growth: A Mathematical Model, *America Journal of Computational and Applied Mathematics*, Vol. 2(6), 276-289.
- Misra, O.P. and Kalra, P. (2013). Effect of Toxic Metal on the Structural Dry Weight of a Plant: A Model, *International Journal of Biomathematics*, Vol. 6 (5), 1350028 (1-27).
- Nwachukwu Olayinka I. and Agbede Olusola O. (2009). Plant Bioaccumulation and Root- To - Shoot Transport of Metals In A Field Soil Contaminated By Mining Activities, Vol.5, 309-319.
- Pugliese, A. (1988). Optimal Resource Allocation in Perennial Plants: A Continuous-Time model, *Theoretical Population Biology*, Vol. 34, No. 3.
- Pishchik,V. N., Vorobyev, N.I., Chernyaeva, I.I., Timofeeva, S.V., Kozhemyakov, A. P., Alexeev, Y. V. and Lukin, S. M. (2002). Experimental and Mathematical Simulation of Plant Growth Promoting Rhizobacteria and Plant Interaction under Cadmium Stress, *Plant and Soil*, Vol. 243, 173-186.
- Somma,F., Hopmans,J.W. and Clausnitzer,V. (1998). Transient Three-Dimensional Modelling of Soil Water and Solute Transport with Simultaneous root Growth, Root Water and Nutrient Uptake, *Plant and soil*, Vol. 202, 281-293.
- Smical, A.I., Hotea, V., Oros, V., Juhasz, J. and Pop, E. (2008). Studies on Transfer and Bioaccumulation of Heavy Metals From Soil into Lettuce, *Environmental Engineering and Management Journal*, Vol. 7, No.5, 609-615.
- Thornley, J.H.M. (1976). Mathematical Models in Plant Physiology, *Academic Press*, NY.
- Thomas, D.M., Vandemeulebroeke, L. and Yamaguchi, K. (2005). A Mathematical Evolution Model for Phytoremediation of Metals, www.csam.montclair.edu.
- Verma, P., George, K. V., Singh, H. V. and Singh, R. N. (2007). Modeling Cadmium Accumulation in Radish, Carrot, Spinach and Cabbage, *Applied Mathematical Modelling*, Vol. 31, 1652-1661.
- Vance, R.R. and Neveai, A.L. (2007). Plant Population Growth and Competition in a Light Gradient : A Mathematical Model of Canopy Partitioning, *Journal of Theoretical Biology*, Vol. 245, 210-219.

Violante, A., Cozzolino, V., Perelomov, L., Caporale, A.G. and Pigna, M. (2010). Mobility and Bioavailability of Heavy Metals and Metalloids in Soil Environments, *J.Soi. Sci. Plant Nutr.* 10(3): 268-292.

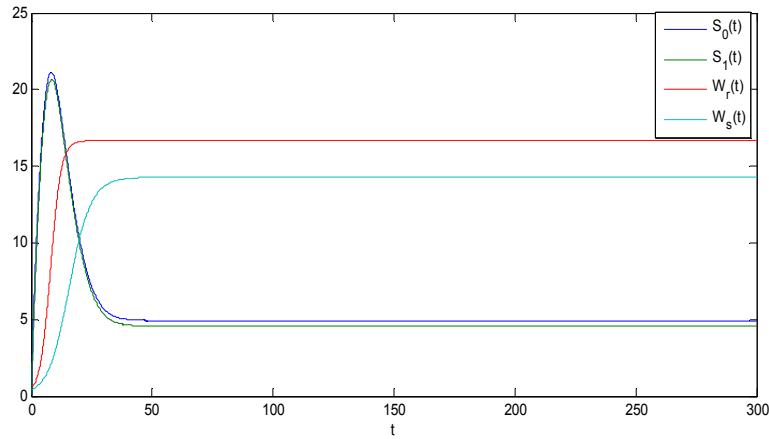


Figure 1. Trajectories of the Model 1 with respect to time (with no toxic effect) showing the stability behaviour

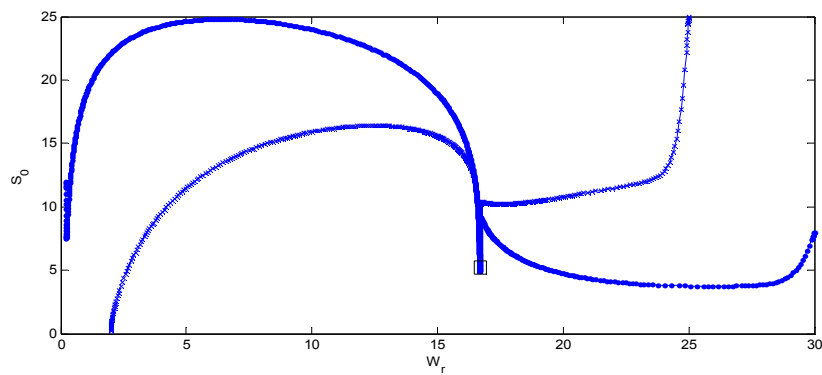


Figure2. Phase plane graph for nutrient concentration in root S_0 and root biomass W_r at different initial conditions given in Table 1 for Model 1 (with no toxic effect) showing the global stability behaviour.

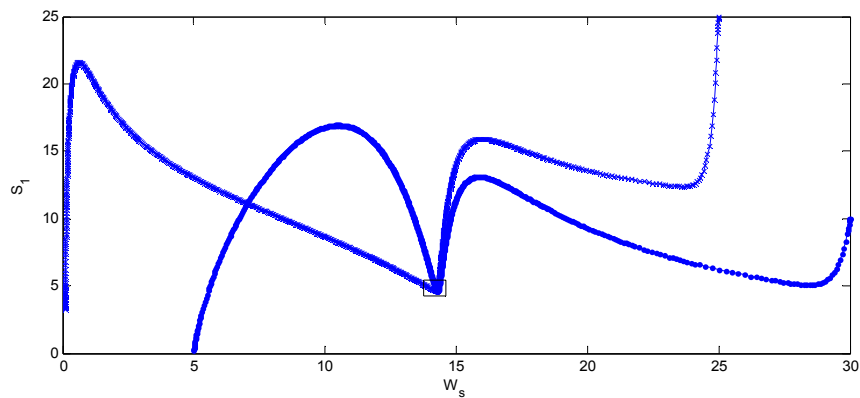


Figure 3. Phase plane graph for nutrient concentration in shoot S_1 and shoot biomass W_s at different initial conditions given in Table 1 for Model 1 (with no toxic effect) showing the global stability behaviour.

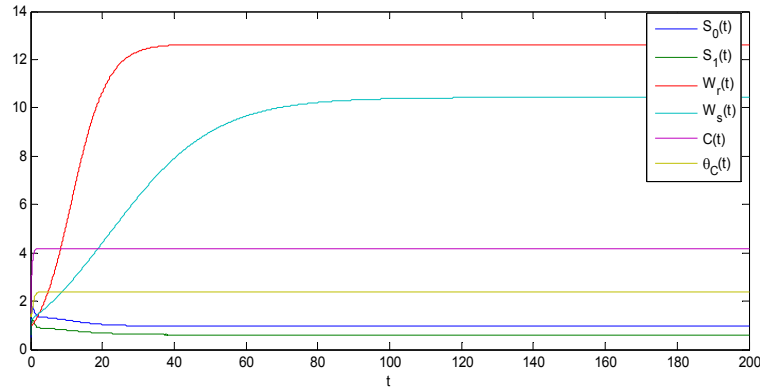


Figure 4. Trajectories of the model 2 with respect to time (with toxic effect) showing the stability behaviour.

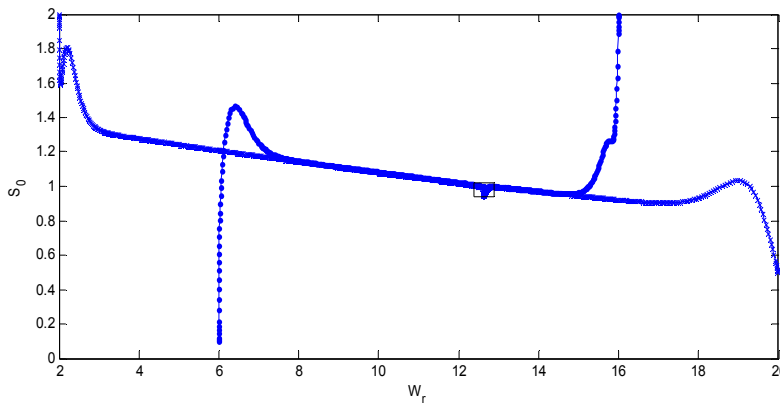


Figure 5. Phase plane graph for nutrient concentration in root S_0 and root biomass W_r at different initial conditions given in Table 3 for Model 2 (with toxic effect) showing the global stability behavior.

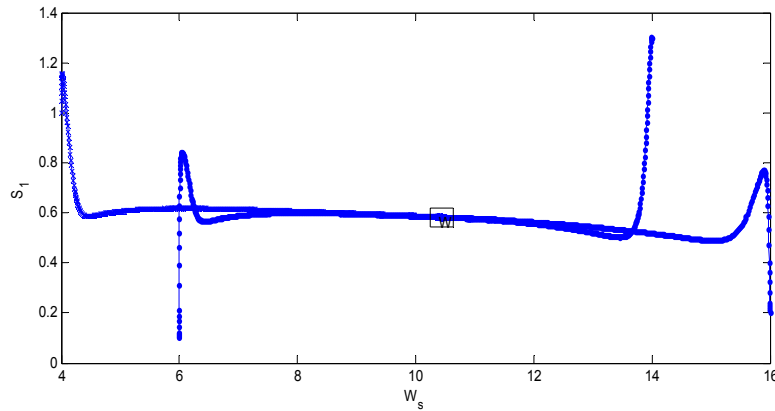


Figure 6. Phase plane graph for nutrient concentration in shoot S_1 and shoot biomass W_s at different initial conditions given in Table 4 for Model 2 (with toxic effect) showing the global stability behaviour.

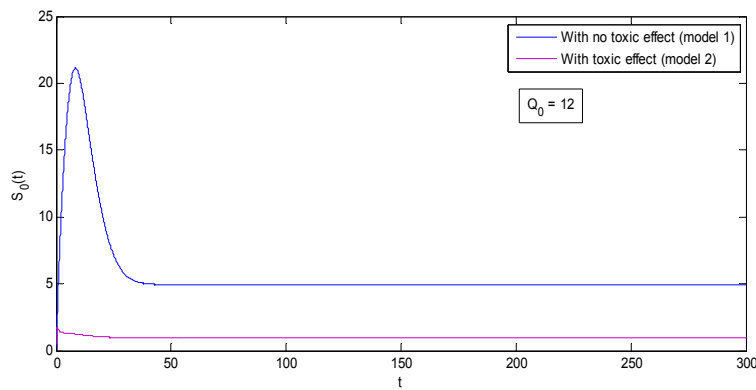


Figure 7(a). Graph between nutrient concentration of root S_0 and time t for Model 1 (with no toxic effect) and for Model 2 (with toxic effect)

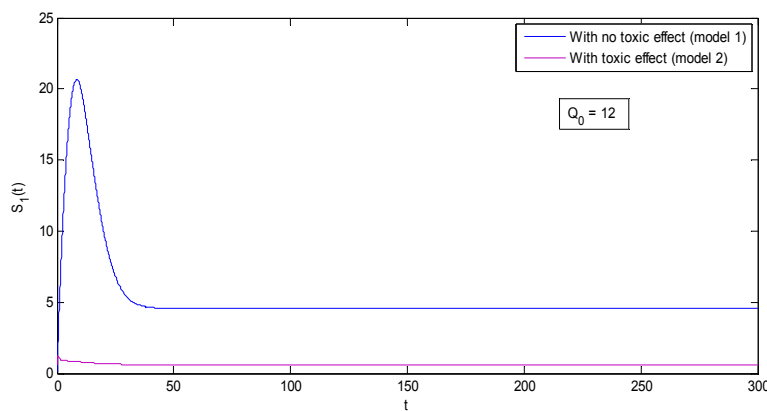


Figure 7(b). Graph between nutrient concentration in shoot S_1 and time t for Model 1 (with no toxic effect) and for Model 2 (with toxic effect)

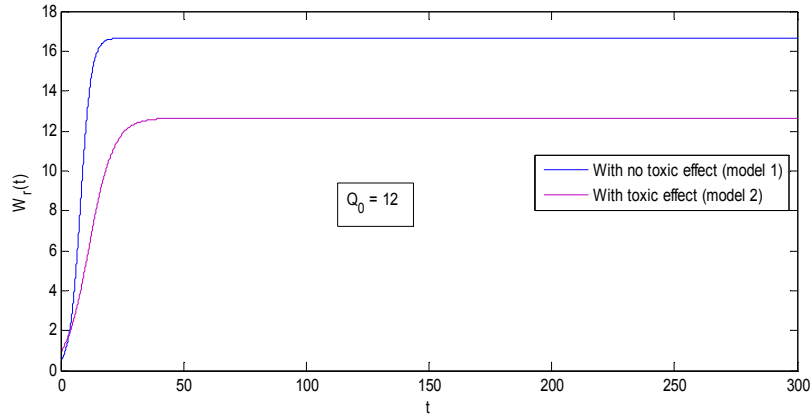


Figure 8(a). Graph between root biomass W_r and time t for Model 1 (with no toxic effect) and for Model 2 (with toxic effect)

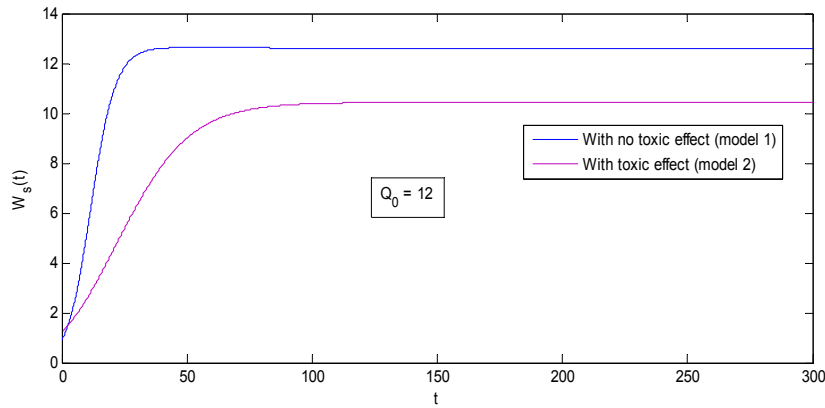


Figure 8(b). Graph between shoot biomass W_s and time t for Model 1 (with no toxic effect) and for Model 2 (with toxic effect).

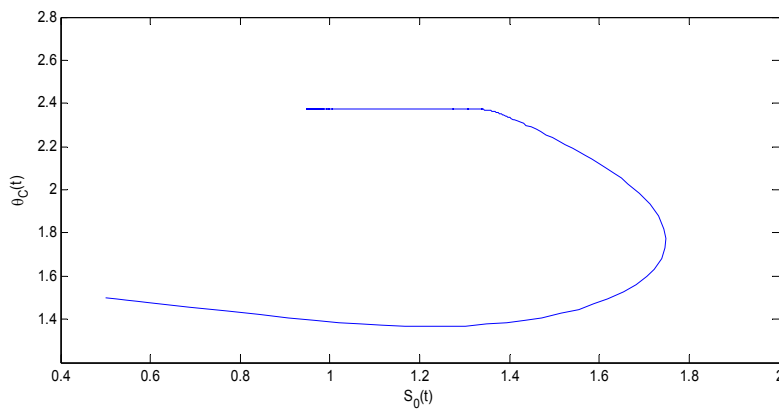


Figure 9(a). Phase Plane Graph of nutrient concentration in root S_0 and θ_c for Model 2 when $Q_0 = 12$.

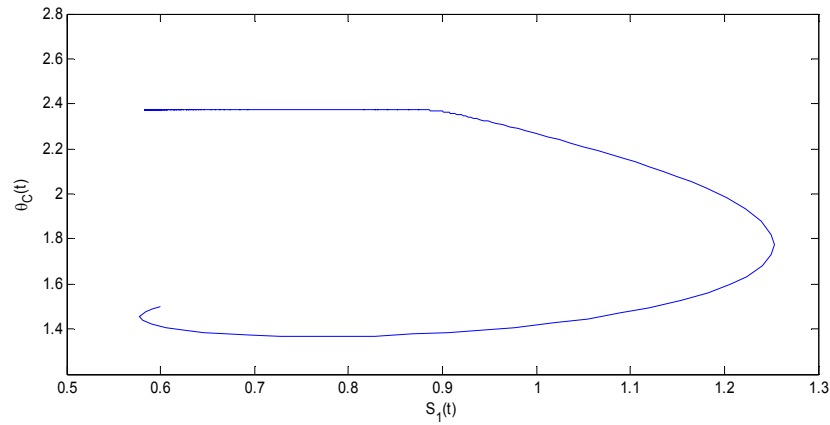


Figure 9(b). Phase Plane Graph of nutrient concentration in shoot S_1 and θ_C for Model 2 when $Q_0 = 12$.